

Nonlinear dynamics of upward propagating flames

Mariam Battikh 


*Technological University of Compiègne, ESCOM, TIMR, rue du Dr Schweitzer, 60200 Compiègne, France
and INERIS, PHDS Department, Parc Technologique ALATA, BP 2, 60550 Verneuil-en-Halatte, France*

Elias Al Sarraf

Faculty of Engineering Branch 1, Lebanese University, Daher EL Ein, 1300 Tripoli, Lebanon

Basile Radisson 

Nonlinear Physical Chemistry Unit, Université libre de Bruxelles (U.L.B.), CP 231, Campus de la Plaine, 1050 Bruxelles, Belgium

Christophe Almarcha and Bruno Denet 

Aix Marseille University, CNRS, Centrale Marseille, IRPHE UMR 7342, 13384 Marseille, France



(Received 14 November 2022; accepted 9 June 2023; published 28 June 2023)

We study the influence of gravity on the dynamics of upward propagating premixed flames. We show that the role of gravity on the dispersion relation is small, but that the nonlinear effects are large. Using a Michelson Sivashinsky equation modified with a gravity term, it can be observed that the nonlinear dynamics of the crests is greatly influenced by gravity, as well as the final amplitude of the flame. A simple model is proposed to explain the role of gravity on the amplitude.

DOI: [10.1103/PhysRevE.107.065110](https://doi.org/10.1103/PhysRevE.107.065110)

I. INTRODUCTION

The propagation of a premixed flame often leads to the development of instabilities. The primary destabilizing effect (Darrieus-Landau instability) [1,2] is modified, as discussed in recent books [3,4], by stabilizing effects (thermal and molecular diffusion within the flame) [5–7] and nonlinearities [8]. In the usual case of downward propagating flames, gravity is also stabilizing. We will be interested in this article in upward propagating flames, where both effects, gravity and Darrieus-Landau instability, participate in wrinkling the flame front.

The problem of upward propagation of premixed flames in a vertical tube is a classical problem. In the 1980s, soon after a correct theory of the Darrieus-Landau instability appeared [5–7], there was also an interest in upward propagating flames. Experiments were performed [9,10] and a theoretical article using a unimodal approximation for the flow field [11] was published. Curiously enough, most of the studies were performed in cases where the Rayleigh-Taylor instability is more important than the Darrieus-Landau instability. In this limit, it was expected that these flames approach the limit of rising bubbles studied by Davies and Taylor [12] when the laminar flame velocity is very low. More recent works exist in this limit [13,14], but a recent theoretical article [15] has however argued that rigorously the propagating flame cannot approach a Taylor bubble even for a very low flame velocity.

Another type of approach has been also initiated in the 1980s by Rakib and Sivashinsky [16] (see also [17]). Instead of considering the laminar flame velocity as a perturbation of a Taylor bubble, this limit corresponds to relatively large laminar flame velocities, so that the gravity effect can be seen

as a perturbation of the (Michelson) Sivashinsky equation of premixed flames [8].

The same type of equation has also been used for downward propagating flames [18–20], and recently this type of equation has been compared to downward propagating flames in a Hele-Shaw cell [21]. It was shown that, although the gravity effect seems small for the linear development of the instability, it helps explain some nonlinear effects, such as the creation of new cells on the front. These creations of new cells cannot be observed with the Sivashinsky equation without gravity term [22,23]. A recent study on the role of gravity in the Michelson-Sivashinsky equation can be found in [24].

At large time of propagation, nonlinear effects have a leading role in the front dynamics. Several theoretical analyses of the nonlinear dynamics of flame fronts have been published either in the limit of small front amplitude [25–27], with the on-shell description of flame fronts [28,29], or in the limit of small gas expansion through the flame $E = \rho_u/\rho_b \rightarrow 1$ [8,30,31]. The latter type of analysis leads to the weakly nonlinear Sivashinsky equation (or sometimes Michelson-Sivashinsky equation):

$$\phi_t + \frac{u_A}{2} \phi_x^2 = \frac{4\sigma_M}{k_c} \left(\frac{\phi_{xx}}{k_c} + I(\phi, x) \right), \quad (1)$$

where ϕ is the local vertical coordinate of the flame front, x is the lateral coordinate, and the position of the front is $[x, \phi(x, t)]$. ϕ_x and ϕ_{xx} are the first and second derivatives with respect to x , ϕ_x^2 is the square of the first derivative, and u_A is a speed that depends on the laminar flame speed and on the density ratio between fresh and burnt gases. σ_M is the growth rate of the most amplified wavelength. k_c is the

cutoff wave number for which the disturbance amplification due to the Darrieus-Landau effect and the damping due to transport into the thickness of the flames cancel out. $I(\phi, x)$ is a linear operator corresponding to multiplication by $|k|$ in Fourier space:

$$I[\cos(kx)] = |k| \cos(kx), \quad I[\sin(kx)] = |k| \sin(kx).$$

We want to incorporate gravity effects into the pseudodifferential Sivashinsky equation (1) in order to take their influence into account in the late time nonlinear dynamics of the flame. We will show in Sec. II that the dispersion relation associated with the Sivashinsky equation can be modified in the presence of gravity in the form

$$\sigma(k) = \frac{4\sigma_M}{k_c} \left(|k| - \frac{k^2}{k_c} \right) + G, \quad \sigma(k=0) = 0, \quad (2)$$

where k and σ are respectively the wave number and the growth rate and G is a parameter controlling the effect of gravity on the dispersion relation. G is positive for upward propagating flames. Note that the maximum growth rate is now $\sigma_M + G$.

Inserting this dispersion relation into the Sivashinsky equation, the obtained equation of Rakib Sivashinsky type (MSG later in this paper) is of the form

$$\phi_t + \frac{u_A}{2} (\phi_x^2 - \langle \phi_x^2 \rangle) = \frac{4\sigma_M}{k_c} \left(\frac{\phi_{xx}}{k_c} + I(\phi, x) \right) + G(\phi - \langle \phi \rangle), \quad (3)$$

which reduces to (1) in the limit $G \rightarrow 0$ through a simple change of frame of reference. Numerical experiments obtained by pseudospectral integration of Eq. (3), reported in Sec. IV, show a strongly modified dynamics (even for $G \ll \sigma_M$) compared to the standard Sivashinsky model.

The purpose of the present work is to study this Rakib Sivashinsky type of equation for upward propagating flames, compare the nonlinear evolution of the front to experiments in a Hele-Shaw cell for short times, and examine how the behavior of the flame for long times is modified by the gravity term.

II. DISPERSION RELATION

A dispersion relation valid for temperature-dependent diffusivities has been proposed by Clavin and Garcia [7] (see also [32]) in the form of a quadratic equation. Note that although we will compare to experiments in a Hele-Shaw burner, we do not present here the dispersion relation in the limit of very small Hele-Shaw cell thickness, which can be found in [33]. The following temperature dependence: $\rho D \propto T^\beta$, with T being the temperature, is often used in the literature; β is often taken to be 0.69 or 0.5. This dispersion relation reads

$$A(k)\sigma^2 + B(k)\sigma + C(k) = 0, \quad (4)$$

with $A(k)$, $B(k)$, and $C(k)$ coefficients depending on gas expansion $E = \rho_u/\rho_b$, Markstein number Ma , Froude number $\text{Fr} = u_l^2/g\delta_l$ (where u_l is the laminar flame speed and $\delta_l = \frac{D_0}{u_l}$ the flame thickness; g is the acceleration of gravity, taken positive for downward propagating flames), and Prandtl

number Pr :

$$\begin{aligned} A(k) &= \frac{E+1}{E} + \frac{E-1}{E} k\delta_l \left(\text{Ma} - J \frac{E}{E-1} \right), \\ B(k) &= u_l k (2 + 2Ek\delta_l (\text{Ma} - J)), \\ C(k) &= u_l^2 \left\{ \frac{E-1}{E} \frac{k}{\text{Fr}\delta_l} + (E-1) \frac{k^3}{k_m} \right. \\ &\quad \left. - (E-1)k^2 \left[1 + \frac{1}{E\text{Fr}} \left(\text{Ma} - J \frac{E}{E-1} \right) \right] \right\}, \quad (5) \end{aligned}$$

where $k_m^{-1} = \delta_l (E^\beta + \frac{3E-1}{E-1} \text{Ma} - \frac{2E}{E-1} J + (2\text{Pr} - 1)H)$. The integrals J and H can be found in [7,32].

This dispersion relation includes explicitly the Froude number, which is of course necessary in our case, where the gravity plays an important role. Note that the buoyancy effect is introduced through the Froude number in the term $C(k)$ only.

The theoretical dispersion relations are only valid for low values of k ; we have shown in [34] that a development of the Clavin-Garcia dispersion relation (we will call this relation modified Clavin-Garcia dispersion relation), valid for $k \ll 2\pi/\delta_l$ and $1/\text{Fr} = O(k)$, gives

$$\sigma = a_g u_l k - b_g k^2, \quad (6)$$

where positive coefficients a_g and b_g are functions of k including Froude number effects.

A development leads to

$$a_g = \frac{E}{E+1} [S_g - 1], \quad (7)$$

where

$$\begin{aligned} S_g &= \sqrt{1 + E - \frac{1}{E} - \frac{E^2 - 1}{E^2 \text{Fr} k \delta_l}} \\ &= \sqrt{1 + E - \frac{1}{E} - \frac{g(E^2 - 1)}{E^2 u_l^2 k}}, \quad (8) \end{aligned}$$

the relation $\sigma = a_g u_l k$ is the Darrieus-Landau result with gravity, but without Markstein number effect, and

$$\begin{aligned} b_g &= -\delta_l u_l \left[\left(-a_g^2 \frac{E-1}{E} - 2a_g E + \frac{E-1}{Ek\text{Fr}\delta_l} \right) \text{Ma} \right. \\ &\quad \left. + J \left(a_g^2 - \frac{1}{k\text{Fr}\delta_l} + 2a_g E \right) - \frac{E-1}{k_m \delta_l} \right] / 2S. \quad (9) \end{aligned}$$

This relation between b_g and the Markstein number is complicated and depends on the temperature dependence of the diffusivities through the integrals J and H . As the precision of the reported Markstein numbers in the literature is very low [34], we prefer in the next section to fit the value of b_g .

For $k=0$, the growth rate given by Eq. (6) is zero. Outside a boundary layer very close to $k=0$, let us develop the square root in Eq. (8) (this development is not valid for extremely small k or small laminar flame velocity). We obtain

$$\sigma = G + a_l k - b_g k^2, \quad \sigma(k=0) = 0, \quad (10)$$

where $a = \frac{E}{E+1}[S-1]$, $S = \sqrt{1+E-\frac{1}{E}}$, and the value of G is given by

$$G = -\frac{1}{2} \frac{(E-1)g}{Eu_l S}, \quad (11)$$

showing that the dispersion relation is of the form given in Eq. (2). Note that for upward propagating flames we have taken g to be negative, so that in this case G is positive. Numerically however G is small (much smaller than the maximum growth rate) for typical values of the laminar flame speed and gas expansion. We will show in the next sections that, although small in the linear regime, G plays an important role in the nonlinear dynamics of the flame and its final amplitude.

III. COMPARISON WITH EXPERIMENTS

The dynamics described by (3) will now be compared to experimental flames. We use here the Hele-Shaw burner employed in our recent studies [23,34–36]. This apparatus is made of two borosilicate glass plates ($1500 \times 500 \times 5$ mm) oriented vertically and separated by a 3.5 mm gap. The burner cavity is opened at the bottom and closed on the two vertical sides, the gas supply being placed at the top of the cell. For the experiments presented in this article, the burner is filled with a propane-air mixture with equivalence ratio $\varphi = 0.9$ through a flow line positioned at the top of the experimental facility and controlled by two Bronkhorst EL-Flow series mass-flow regulators. Before flame ignition, the flow rate of the mixture is adjusted so that the speed of the flow at the bottom outlet of the burner is slightly in excess to the flame speed. This technique allows the flame to remain anchored at the bottom of the burner as a two-dimensional (2D) Bunsen flame. After ignition of the flame, the mixture flow is then suddenly stopped and the flame starts its upward propagation. Experiments are performed with a forcing using plates with a sinusoidal shape at the bottom allowing one to force modes of different wavelengths and to measure their growth rates using image analysis. The experimental values of the growth rate are fitted with a Levenberg-Marquardt algorithm: a two-parameter fit is performed using the modified Clavin-Garcia formula [Eqs. (6) and (7)] (u_l taken to its experimental value in tubes), giving the two parameters (E , b_g). As usual in experiments in Hele-Shaw burners, heat losses lead to a value of E lower than the value for flames propagating in tubes. The results of this fit compared to experimental values of growth rates for upward propagating flames are shown in Fig. 1. With the growth rates being higher for upward propagating flames compared to downward propagating flames, the measured values are generally less precise than in the downward case. Nevertheless, Fig. 1 shows that the fit with the modified Clavin-Garcia dispersion relation is in reasonable agreement with the experiments.

The modified Clavin-Garcia relation shown in Fig. 1 is then expanded according to Eq. (11) giving the value of G and the dispersion relation used in the MSG equation. A flame front is extracted from experiments using image processing as described in [34,35] and is used as an initial condition $\phi(x, t = 0)$ for a direct numerical simulation of Eq. (3). The integration is performed by a pseudospectral spatial discretization with periodic boundary conditions using the fast Fourier trans-

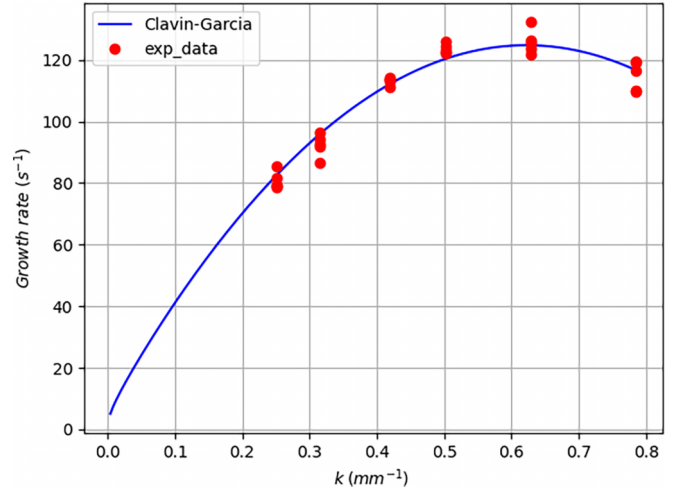


FIG. 1. Experimental growth rates for an upward propagating flame (propane-air flame with equivalence ratio $\varphi = 0.9$), compared to a fit with the modified Clavin-Garcia dispersion relation (parameters $u_l = 391$ mm s⁻¹, $E = 4.21$, and $b_g = 313.6$ mm²s⁻¹).

form library fftw [37]. The time derivatives are discretized using first order finite differences. Details on the numerical method are given in the Appendix. The obtained evolution for the flame front is compared with experiment in Fig. 2. In this figure, the experimental evolution is shown on the left (the flame propagates upward) and the numerical solutions on the right of the figure. A good agreement is observed during the development of the first cells observed on the front and the first mergings of cells. Then, as time evolves, the agreement deteriorates, the main cause being that there is a discrepancy close to the boundary conditions (which are of course not periodic in the experiments). We will show in Sec. IV that the gravity term accelerates the merging of cells.

IV. NONLINEAR EFFECTS OF THE GRAVITY TERM

We have seen in the previous section that we have a good agreement of the MSG equation with experiments for short times. However, it is difficult to study experimentally the late time behavior of flame fronts in our Hele-Shaw cell. With the width we use the flame does not reach a stationary shape during its propagation from the bottom to the top of the cell and there is of course the problem that, by varying the equivalence ratio or the dilution, all the parameters of the dispersion relation [Eq. (2)] are modified. So in this section we turn to numerical simulations of the MSG equation with varying G , with the other parameters used in the simulation being fixed to $\sigma_M = 67$ s⁻¹, $k_c = 0.89$ mm⁻¹, and $u_A = 632.7$ mm s⁻¹, and corresponding to a propane-air flame with equivalence ratio $\varphi = 0.8$ (the numerical values of the parameters are taken from [21]). The MSG equation is solved on $[0, \Lambda]$ with periodic boundary conditions $\Lambda = 158$ mm.

We want to know if a stationary solution is obtained for late time for upward propagating flames and if the amplitude [we will talk of flame brush, defined by $\max(\phi) - \min(\phi)$, where the maximum and minimum are taken over the width of the front, at a given time step] depends in an important

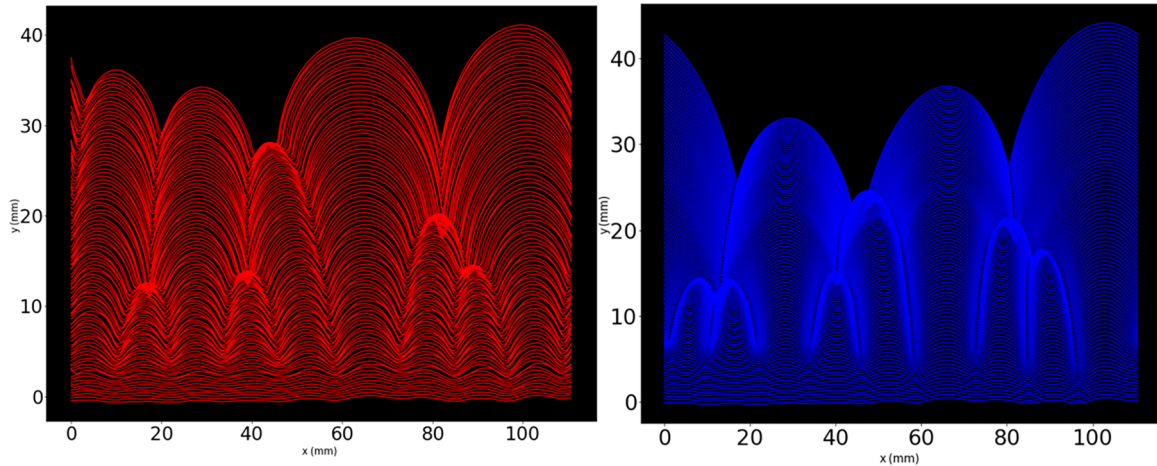


FIG. 2. Nonlinear evolution for an upward propagating flame (propane-air flame with equivalence ratio $\phi = 0.9$). Left: experiment; right: numerical simulation. Wavelength of initial forcing: 12.5 mm. Parameters $\sigma_M = 120 \text{ s}^{-1}$, $k_c = 1.22 \text{ mm}^{-1}$, and $G = 4.29 \text{ s}^{-1}$. x and y are plotted in mm. The lines seen in the figure correspond to the flame fronts at different time steps.

way on G . In Fig. 3 we show simulations of flames for different G . Although we have included cases for negative G and $G = 0$ to compare with upward propagating flames, we present all the cases with the flame propagating from the bottom to the top of the figure. We take as initial condition for all cases a flame with small cells and see the different nonlinear evolution in all four cases $G = -1 \text{ s}^{-1}$, $G = 0 \text{ s}^{-1}$, $G = 1 \text{ s}^{-1}$, and $G = 4 \text{ s}^{-1}$. In all cases the nonlinear evolution first leads to a merging of the initial small cells, but it can be seen that this merging process is accelerated for upward propagating flames and slowed for downward propagating flames compared to the reference case $G = 0$. Furthermore, although $G \ll \sigma_M$ in all cases, the merging of cells is much faster for positive G (upward propagating flames). The late

time behavior is also very different for downward or upward propagating flames. For $G = -1 \text{ s}^{-1}$ we observe in agreement with [21] that new cells are constantly created on the front; this is probably caused by secondary instabilities of the type reported in [20]. For $G = 0 \text{ s}^{-1}$ apparently no instabilities of the curved flame are observed but the flame is very sensitive to noise. For upward propagating flames $G = 1 \text{ s}^{-1}$ and $G = 4 \text{ s}^{-1}$, the curved flame seems more robust and we observe the evolution toward a stationary solution. However, the amplitude of the final solution (the flame brush, as defined before) is completely changed for higher G .

In Fig. 4 the time evolution of the flame brush is plotted for different values of G ($G > 0 \text{ s}^{-1}$ and $G = 0 \text{ s}^{-1}$, which actually tends slowly toward a stationary solution). In this

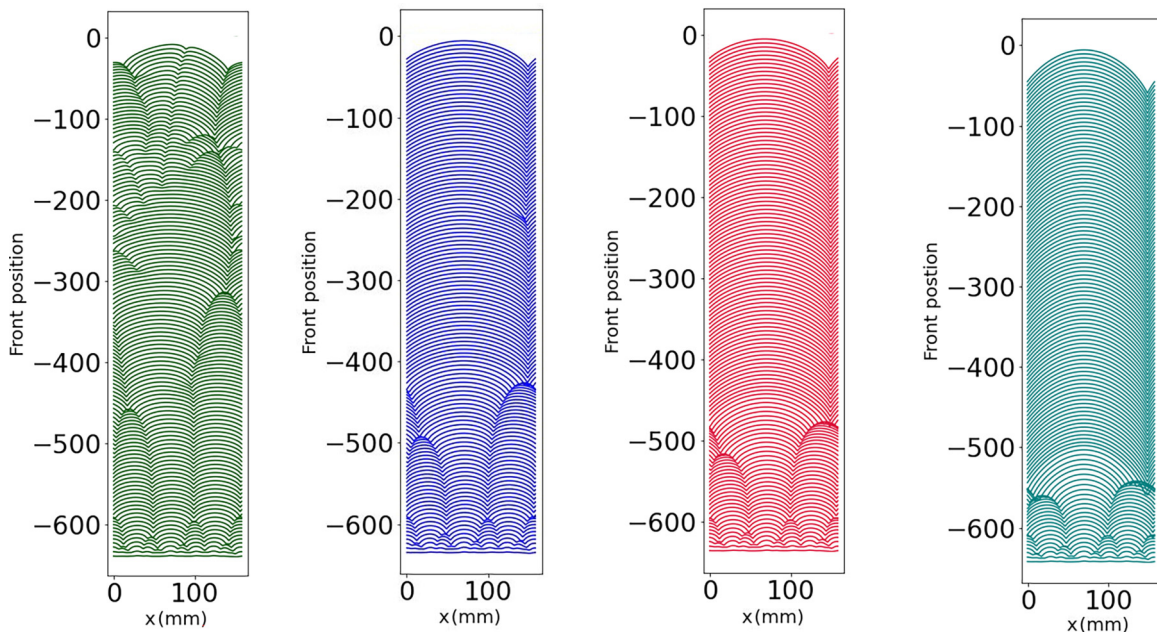


FIG. 3. Simulations of the MSG equation with parameters $\sigma_M = 67 \text{ s}^{-1}$, $k_c = 0.89 \text{ mm}^{-1}$, and from left to right $G = -1 \text{ s}^{-1}$, $G = 0 \text{ s}^{-1}$, $G = 1 \text{ s}^{-1}$, and $G = 4 \text{ s}^{-1}$. x and y are plotted in mm. The front position is defined here as ϕ plus some constant such as the mean flame position increases linearly with time (in the same way for each value of G , to make the comparison easier).

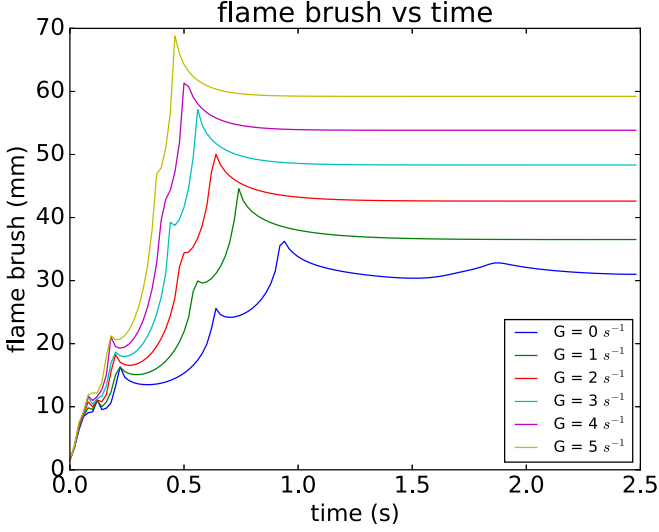


FIG. 4. Flame brush versus time with parameters $\sigma_M = 67 \text{ s}^{-1}$, $k_c = 0.89 \text{ mm}^{-1}$, for different G . The theoretical value of the flame brush given by Eq. (18) for $G = 0 \text{ s}^{-1}$ is 28.0 mm.

figure (see also Fig. 3) we can see the different mergings of the cells at the beginning of the simulation, which correspond to the different maxima of the flame brush versus time. Actually this merging is not too different for the first cells (it can also be seen in Fig. 3) but is strongly accelerated for higher values of G when the cells become larger. At the end of the simulation, a stationary solution is obtained but with a final amplitude which varies almost linearly with G .

To understand this dependency of the final flame brush on G , let us compare to the following equation already proposed by Rakib and Sivashinsky:

$$\phi_t + \frac{u_A}{2} (\phi_x^2 - \langle \phi_x^2 \rangle) = G(\phi - \langle \phi \rangle), \quad (12)$$

which is essentially the MSG equation without the Darrieus Landau and diffusive terms, but where the gravity term has been kept. It has been shown that a simple parabolic solution to this equation exists on $[0, \Lambda]$ in the steady case [16,17,38]

$$\phi = \frac{G}{2u_A} (x - \Lambda/2)^2, \quad (13)$$

which is easily verified by direct substitution into Eq. (12). This leads to a flame brush:

$$\Delta\phi = \frac{G\Lambda^2}{8u_A}. \quad (14)$$

Let us compare this flame brush to the Sivashinsky equation without gravity term. The Sivashinsky equation on $[0, \Lambda]$ can be rescaled to a form often used on $[0, 2\pi]$ in the following way [23]:

$$\begin{aligned} \tau &= \frac{8\pi\sigma_M}{\Lambda k_c} t, \\ X &= \frac{2\pi}{\Lambda} x, \\ \Phi &= \frac{u_A k_c \pi}{2\Lambda\sigma_M} \phi. \end{aligned} \quad (15)$$

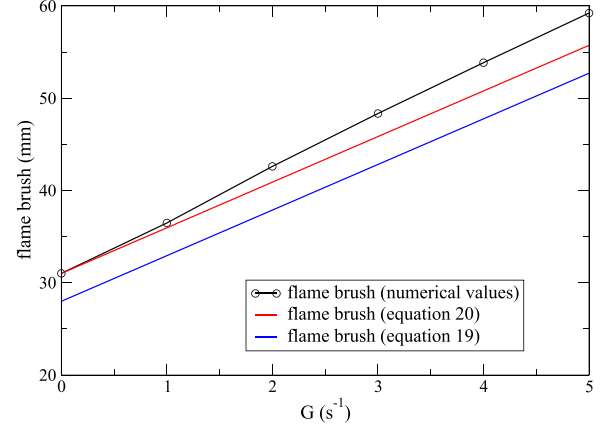


FIG. 5. Flame brush for different G . Upper curve: numerical simulations; lower curve: Eq. (19); middle curve: Eq. (20).

Equation (1) is reduced to a one parameter equation on $[0, 2\pi]$:

$$\Phi_\tau + \frac{1}{2}\Phi_X^2 = \nu\Phi_{XX} + I(\Phi, X), \quad (16)$$

where $1/\nu = k_c/K$ (with $K = 2\pi/\Lambda$) is a parameter corresponding to the ratio of the width of the domain to the shortest unstable wavelength. This parameter, called the unstable modes number, is the only nondimensional number governing the flame dynamics when gravity is neglected. Without the diffusive term, the Sivashinsky equation on $[0, 2\pi]$ has the following solution for the slope [39,40]:

$$\Phi_X = -2/\pi \sinh^{-1}[1/\tan(X/2)]. \quad (17)$$

There is no closed form for Φ ; however, it can be integrated numerically, giving the flame brush $\Delta\Phi$ on $[0, 2\pi]$ and

$$\Delta\phi = \Delta\Phi \frac{2\Lambda\sigma_M}{u_A k_c \pi}, \quad (18)$$

so we see that the Sivashinsky equation without gravity term gives a flame brush proportional to Λ , contrary to Eq. (12), which gives a flame brush proportional to $G\Lambda^2$. Although G is small, for sufficiently large values of Λ , the flame brush can be modified in an important way by the gravity term; this is what is observed in Fig. 4. Of course this reasoning is rather qualitative, but it has been suggested in [38] that it could be reasonable to simply add solutions to Eqs. (1) and (12), so let us compare to numerical simulations

$$\Delta\phi = \Delta\Phi \frac{2\Lambda\sigma_M}{u_A k_c \pi} + \frac{G\Lambda^2}{8u_A}. \quad (19)$$

The first term of this formula is related to the solution of the Sivashinsky equation without diffusivity, which is already an approximation of the solution without gravity. To focus on the effect of gravity, we can also compare to numerical simulations

$$\Delta\phi = \Delta\phi(G=0) + \frac{G\Lambda^2}{8u_A}. \quad (20)$$

In Fig. 5 the flame brushes obtained in the numerical simulations are plotted for various G , with Eqs. (19) and (20) showing that we have a reasonable semiquantitative agreement and with a 10% error associated to the Sivashinsky

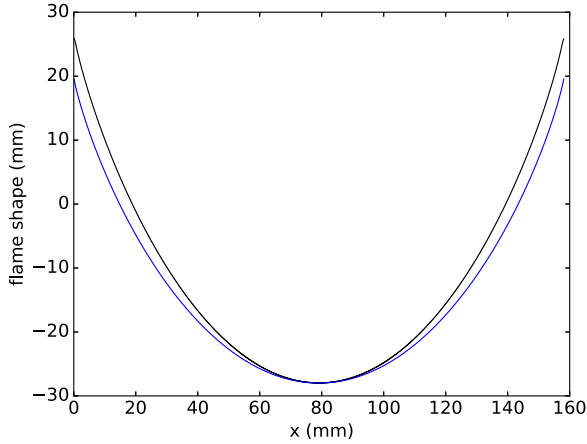


FIG. 6. Front shapes for $G = 4 \text{ s}^{-1}$. Upper curve: numerical simulation; lower curve: theoretical model.

equation flame brush (the number of unstable modes in the domain is 22.4) and another 10% error associated to the gravity term for our larger value $G = 5 \text{ s}^{-1}$. In order to give an idea of the shapes obtained for the flame front, we compare in Fig. 6 the shape obtained numerically for $G = 4 \text{ s}^{-1}$ to the shape obtained by adding ϕ obtained by integrating Eq. (17) (Sivashinsky equation without diffusivity) and the parabolic shape of Eq. (13), showing a relatively good agreement.

To summarize, Eq. (19) contains the main effects observed numerically, almost linear dependence of the amplitude, and large effect of a small value of G . Furthermore, it leads to a physical interpretation, the amplitude caused by gravity is proportional to Λ^2 , and the amplitude caused by the Darrieus-Landau instability is proportional to Λ . However, the fact that Eq. (19) works well quantitatively is surprising.

For larger values of G [i.e., lower flame speeds; see Eq. (11)] the Sivashinsky approximation will not be valid anymore at some point and one should have to use the on-shell method of Kazakov in [15] which is valid when the slope becomes very large, contrary to the present work. For large values of G , the development of the square root in Eq. (8) will not be possible and the dispersion relation will be close to the Rayleigh-Taylor result $\sigma \approx \sqrt{gk}$. In this case, the flame shape will be close to a Taylor bubble [14].

V. CONCLUSION

In this article, we have studied the behavior of upward propagating flames with a modified Sivashinsky equation including a gravity term.

(i) We have shown that a dispersion relation of the type

$$\sigma(k) = \frac{4\sigma_M}{k_c} \left(|k| - \frac{k^2}{k_c} \right) + G \quad (21)$$

is obtained even for realistic gas expansion.

(ii) Inserting this dispersion relation in the modified Sivashinsky equation, we were able to compare the nonlinear evolution to experiments, with a good agreement.

(iii) For longer times, a numerical study showed two effects—a large dependency of the amplitude on G and an accelerated merging of the cells for higher values of G .

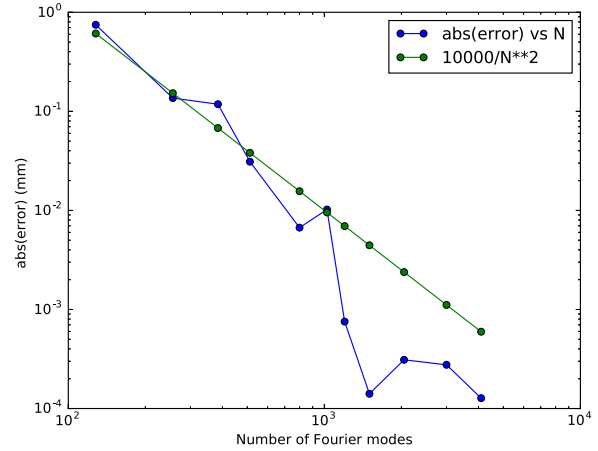


FIG. 7. Error in the amplitude versus number of Fourier modes, in log-log scale for $G = 4 \text{ s}^{-1}$.

(iv) It was possible to explain qualitatively the effect of G on the amplitude with a simple model.

The analysis, however, does not contain the limiting case of very low laminar flame velocity, where the shape of the flame can approach a Taylor bubble, and it would be interesting to describe the transition of the modified Sivashinsky equation to this regime.

ACKNOWLEDGMENTS

We would like to thank G. Joulin and J. Quinard for many stimulating discussions.

APPENDIX: DETAILS ON THE NUMERICAL METHOD

For a flame front ϕ we can define the spectrum (coefficients in Fourier space) $\hat{\phi}$. The superscript n corresponds to the time step $n\Delta t$. The nonlinear term of the MSG equation is computed by a pseudospectral method, i.e., first in physical space before being transformed to the Fourier space to give $\hat{\phi}_x^{2n}$. The numerical scheme (first order in time) is

$$\frac{\hat{\phi}^{n+1} - \hat{\phi}^n}{\Delta t} + (u_A/2)\hat{\phi}_x^{2n} = \sigma(k)\hat{\phi}^{n+1}, \quad (A1)$$

where $\sigma(k)$ is the dispersion relation given in Eq. (2).

This numerical scheme has the usual properties of Fourier spectral methods, no linear system to solve although the scheme is implicit on the linear terms, and high precision (exponential convergence for smooth functions (see Boyd [41], Sec. 2.3) for the spatial derivatives. Nevertheless, the gravity term leads to very stiff cusps, very close to a slope discontinuity, where the spectrum decreases only algebraically in $1/N^2$, where N is the number of Fourier modes, as discussed in the book of Boyd [41], Sec. 2.2.

We give in Fig. 7 the error, defined as the difference of the amplitude of the stationary solutions for $G = 4 \text{ s}^{-1}$ (see Figs. 5 and 6) (with simulations performed with a time step $\Delta t = 10^{-5} \text{ s}$, as in the rest of the paper) for different values of N , with the amplitude for $N = 8192$ (53.846 mm). Although the error decreases slowly with N and there is some noise, it can be seen that the error is smaller than 10^{-3} mm

for a large number of Fourier modes. We use usually 4096 modes in the simulations presented in this paper. Naturally, as the 1D MSG equation describes the same phenomena as

a 2D direct numerical simulation, the calculations are much less expensive than with a 2D DNS, such as in the work of Higuera [14].

-
- [1] G. Darrieus, Propagation d'un front de flamme, *La Technique Moderne* **30**, 18 (1938).
- [2] L. D. Landau, On the theory of slow combustion, *Acta Phys.* **19**, 77 (1944).
- [3] P. Clavin and G. Searby, *Combustion Waves and Fronts in Flows: Flames, Shocks, Detonations, Ablation Fronts and Explosion of Stars* (Cambridge University Press, Cambridge, UK, 2016).
- [4] M. A. Liberman, *Combustion Physics* (Springer, New York, 2021).
- [5] P. Pelcé and P. Clavin, Influence of hydrodynamics and diffusion upon the stability limits of laminar premixed flames, *J. Fluid Mech.* **124**, 219 (1982).
- [6] M. Matalon and B. J. Matkowsky, Flames as gasdynamic discontinuities, *J. Fluid Mech.* **124**, 239 (1982).
- [7] P. Clavin and P. Garcia, The influence of the temperature dependence of diffusivities on the dynamics, *J. Mécanique Théorique et Appliquée* **2**, 245 (1983).
- [8] G. I. Sivashinsky, Nonlinear analysis of hydrodynamic instability in laminar flames—I. Derivation of basic equations, *Acta Astronaut.* **4**, 1177 (1977).
- [9] J. Jarosinski, R. A. Strehlow, and A. Azarbarzin, The mechanisms of lean limit extinguishment of an upward and downward propagating flame in a standard flammability tube, in *Symposium (International) on Combustion* (Elsevier, Amsterdam, 1982), Vol. 19, pp. 1549–1557.
- [10] C. Pelcé-Savornin, J. Quinard, and G. Searby, The flow field of a curved flame propagating freely upwards, *Combust. Sci. Technol.* **58**, 337 (1988).
- [11] P. Pelcé, Effect of gravity on the propagation of flames in tubes, *J. Phys.* **46**, 503 (1985).
- [12] R. M. Davies and G. I. Taylor, The mechanics of large bubbles rising through extended liquids and through liquids in tubes, *Proc. R. Soc. London A* **200**, 375 (1950).
- [13] Y. M. Shtemler and G. I. Sivashinsky, On upward propagating flames, *Combust. Sci. Technol.* **102**, 81 (1994).
- [14] F. J. Higuera, Numerical simulation of the upward propagation of a flame in a vertical tube filled with a very lean mixture, *Combust. Flame* **158**, 885 (2011).
- [15] K. A. Kazakov, Premixed flame propagation in vertical tubes, *Phys. Fluids* **28**, 042103 (2016).
- [16] Z. Rakib and G. I. Sivashinsky, Instabilities in upward propagating flames, *Combust. Sci. Technol.* **54**, 69 (1987).
- [17] A. B. Mikishev and G. I. Sivashinsky, Quasi-equilibrium in upward propagating flames, *Phys. Lett. A* **175**, 409 (1993).
- [18] B. Denet, On non-linear instabilities of cellular premixed flames, *Combust. Sci. Technol.* **92**, 123 (1993).
- [19] B. Denet and J.-L. Bonino, Laminar premixed flame dynamics: A comparison of model and complete equations, *Combust. Sci. Technol.* **99**, 235 (1994).
- [20] B. Denet, Intrinsic instabilities of curved premixed flames, *Europhys. Lett.* **21**, 299 (1993).
- [21] B. Radisson, B. Denet, and C. Almarcha, Nonlinear dynamics of flame fronts with large-scale stabilizing effects, *Phys. Rev. E* **103**, 063104 (2021).
- [22] C. Almarcha, B. Radisson, E. Al Sarraf, E. Villermaux, B. Denet, and J. Quinard, Interface dynamics, pole trajectories, and cell size statistics, *Phys. Rev. E* **98**, 030202(R) (2018).
- [23] B. Radisson, B. Denet, and C. Almarcha, Nonlinear dynamics of premixed flames: from deterministic stages to stochastic influence, *J. Fluid Mech.* **903**, A17 (2020).
- [24] K. Matsue and M. Matalon, Dynamics of hydrodynamically unstable premixed flames in a gravitational field—local and global bifurcation structures, *Combust. Theory Model.* **27**, 346 (2023).
- [25] V. V. Bychkov, Nonlinear equation for a curved stationary flame and the flame velocity, *Phys. Fluids* **10**, 2091 (1998).
- [26] V. V. Bychkov and A. Kleev, The nonlinear equation for curved flames applied to the problem of flames in cylindrical tubes, *Phys. Fluids* **11**, 1890 (1999).
- [27] V. V. Bychkov and M. A. Liberman, Dynamics and stability of premixed flames, *Phys. Rep.* **325**, 115 (2000).
- [28] K. A. Kazakov, On-shell description of stationary flames, *Phys. Fluids* **17**, 032107 (2005).
- [29] G. Joulin, H. El-Rabii, and K. A. Kazakov, On-shell description of unsteady flames, *J. Fluid Mech.* **608**, 217 (2008).
- [30] G. I. Sivashinsky and P. Clavin, On the nonlinear theory of hydrodynamic instability in flames, *J. Phys.* **48**, 193 (1987).
- [31] G. Joulin and P. Cambray, On a tentative, approximate evolution equation for markedly wrinkled premixed flames, *Combust. Sci. Technol.* **81**, 243 (1992).
- [32] J.-M. Truffaut and G. Searby, Experimental study of the Darrieus-Landau instability on an inverted-V flame, and measurement of the Markstein number, *Combust. Sci. Technol.* **149**, 35 (1999).
- [33] D. Fernández-Galisteo and V. N. Kurdyumov, Impact of the gravity field on stability of premixed flames propagating between two closely spaced parallel plates, *Proc. Combust. Inst.* **37**, 1937 (2019).
- [34] E. Al Sarraf, C. Almarcha, J. Quinard, B. Radisson, B. Denet, and P. Garcia-Ybarra, Darrieus–Landau instability and Markstein numbers of premixed flames in a Hele-Shaw cell, *Proc. Combust. Inst.* **37**, 1783 (2019).
- [35] E. Al Sarraf, C. Almarcha, J. Quinard, B. Radisson, and B. Denet, Quantitative analysis of flame instabilities in a Hele-Shaw burner, *Flow, Turbul. Combust.* **101**, 851 (2018).
- [36] M. Tayyab, B. Radisson, C. Almarcha, B. Denet, and P. Boivin, Experimental and numerical lattice-Boltzmann investigation of the Darrieus-Landau instability, *Combust. Flame* **221**, 103 (2020).
- [37] <http://www.fft.w.org/>.

- [38] G. Boury, Etudes Théoriques et Numériques de Fronts de Flammes Plissées: Dynamiques Non-Linéaires Libres Ou Bruitées, Ph.D. thesis, Université de Poitiers, 2003.
- [39] G. Joulin and B. Denet, Shapes and speeds of steady forced premixed flames, [Phys. Rev. E **89**, 063001 \(2014\)](#).
- [40] G. Joulin and B. Denet, Sivashinsky equation for corrugated flames in the large-wrinkle limit, [Phys. Rev. E **78**, 016315 \(2008\)](#).
- [41] J. P. Boyd, *Chebyshev and Fourier Spectral Methods* (Courier Corporation, New York, 2001).